JOURNAL OF Materials CHEMISTRY

Organic light-emitting diodes using a novel family of amorphous molecular materials containing an oligothiophene moiety as colour-tunable emitting materials

Tetsuya Noda, Hiromitsu Ogawa, Naoki Noma and Yasuhiko Shirota*

Department of Applied Chemistry, Faculty of Engineering, Osaka University, Yamadaoka, Suita, Osaka 565–0871, Japan. E-mail: shirota@ap.chem.eng.osaka-u.ac.jp

Received 8th April 1999, Accepted 16th June 1999

A novel family of amorphous molecular materials containing an oligothiophene moiety with varying conjugation length function as thermally and morphologically stable, colour-tunable emitting materials for organic light-emitting diodes (LEDs). Tuning of the emission colour from light blue to orange is achieved by varying the conjugation length of the oligothiophene moiety. Double-layer organic LEDs that use this novel class of amorphous molecular materials as an emitting layer and tris(quinolin-8-olato)aluminium or 1,3,5-tris[5-(4-*tert*-butylphenyl)-1,3,4-oxadiazol-2-yl]benzene as an electron-transport layer exhibit high performances.

Introduction

Organic light-emitting diodes (LEDs) have been receiving a great deal of attention in view of their application to full-colour flat-panel displays. There have been extensive studies of organic LEDs with the aim of achieving high brightness and multicolour emission, and improving the durability of devices. Both low molecular-weight organic materials[1] and polymers[2] have been studied for use as materials in organic LEDs. We have performed a series of studies of organic LEDs using amorphous molecular materials,[3–24] which include the creation of novel families of thermally and morphologically stable hole-transporting amorphous molecular materials,[4–8,10,12,14] electron-transporting amorphous molecular materials[12,23] and emitting amorphous molecular materials,[15,17,18,24] fabrication of thermally stable organic LEDs,[10,11,13,14] durable organic LEDs[9,12] and blue-emitting organic LEDs,[15,24] colour tuning using exciplex formation at the interface between the hole-transport layer and the electron-transport layer,[20–22] *etc*.

With regard to low molecular-weight organic emitting materials, tris(quinolin-8-olato)aluminium (Alq_3) has been used most extensively as a green-emitting material with electron-transporting properties.[1] Other emitting materials include bis(benzo[*h*]quinolin-10-olato)beryllium as a green emitter[25] and 4,4′-bis(2,2-diphenylethenyl)biphenyl,[26] 3-(biphenyl-4-yl)-4-(4-ethylphenyl)-5-(4-dimethylamino)-1,2,4-triazole,[27] tri(*p*-terphenyl-4-yl)amine,[15] 2,2′,7,7′-tetrakis(biphenyl-4-yl)-9,9′-spirobifluorene,[28] and 5,5′-bis(dimesitylboryl)-2,2′-bithiophene[24] as blue emitters.

Oligothiophenes with well-defined structures, *e.g.*, unsubstituted and alkyl- or silyl-substituted pentamer, hexamer, and heptamer, have also been studied for use as emitting materials in organic LEDs; however, the performances of organic LEDs[29–32] using oligothiophenes as emitting materials are poor. Oligothiophenes are crystalline in nature and hence they form polycrystalline films by a vacuum deposition or spin-coating method.[33,34] The fluorescence quantum efficiencies of oligothiophenes are significantly reduced in going from a solution to a polycrystalline film.

Creation of amorphous molecular materials containing an oligothiophene moiety is of great interest from the following viewpoints. They may constitute a new class of amorphous molecular materials. It is expected that their fluorescence quantum efficiencies may not be significantly reduced in the amorphous film and hence they are expected to function as good emitting materials for organic LEDs, permitting colour tuning through control of the conjugation length. In the light of these considerations, we have designed and synthesised a novel family of π-electron systems containing an oligothiophene moiety, 2,5-bis{4-[bis(4-methylphenyl)amino]phenyl}-thiophene (BMA-1T), 5,5′-bis{4-[bis(4-methylphenyl)-amino]phenyl}-2,2′-bithiophene (BMA-2T), 5,5″-bis{4-[bis(4-methylphenyl)amino]phenyl}-2,2′:5′,2″-terthiophene (BMA-3T), and 5,5‴-bis{4-[bis(4-methylphenyl)amino]phenyl}-2,2′:5′,2″:5″,2‴-quarterthiophene (BMA-4T), and found that these compounds readily form stable amorphous glasses with high glass-transition temperatures (T_gs) when the melt samples are cooled.[16]

We have reported the fabrication and performances of single-layer organic LEDs using this novel family of amorphous molecular materials, BMA-*n*T ($n=1$–4), as emitting materials. Tuning of the emission colour from light blue to orange is achieved by varying the conjugation length ($n=1$–4) of the oligothiophene moiety.[18]

We report here the fabrication and performances of double-layer organic LEDs that use BMA-*n*T ($n=1$–4) as emitting materials with hole-transporting properties and Alq_3 or 1,3,5-tris[5-(4-*tert*-butylphenyl)-1,3,4-oxadiazol-2-yl]benzene (TPOB) as electron-transporting materials, which exhibit much higher performances than the single-layer devices. A double-layer device using BMA-3T and Alq_3 has been reported in our previous communication.[17] In the present paper, performances of organic LEDs using emitting amorphous molecular materials, BMA-*n*T ($n=1$–4), are discussed with reference to those of organic LEDs using polycrystalline oligothiophenes and with respect to the structure of the device, *i.e.*, single-layer and double-layer structures.

Experimental

BMA-*n*T ($n=1$–4) were synthesised by the Grignard coupling reaction of 4-bromophenylbis(4-methylphenyl)amine with the corresponding dibromooligothiophene, as described in our previous communication.[16] They were identified by IR, ^{1}H NMR and electronic absorption spectroscopies, mass spectrometry, and elemental analysis. Alq_3 was prepared by the reaction of quinolin-8-ol with aluminium chloride hexahydrate in NaOH aqueous solution at room temperature and purified by sequential sublimation. TPOB was synthesised by a ring closure reaction of 1,3,5-tris[3-(4-*tert*-butylbenzoyl)carbazoyl]-benzene with $POCl_3$, purified by silica-gel column chromatog-

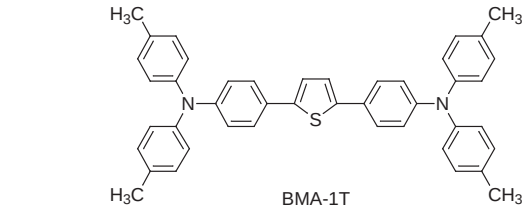

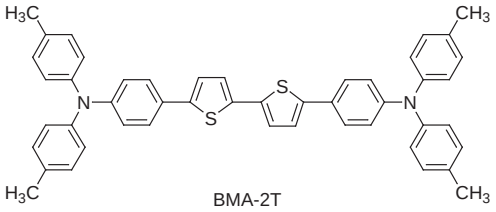

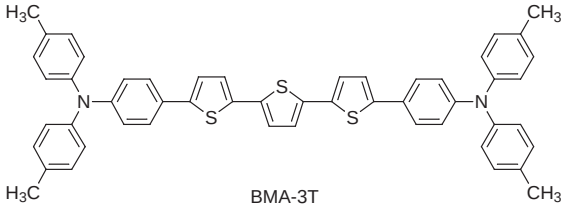

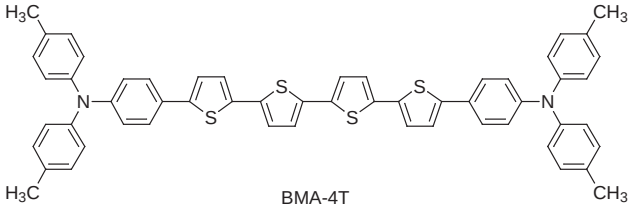

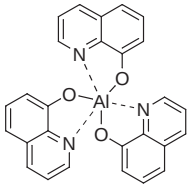

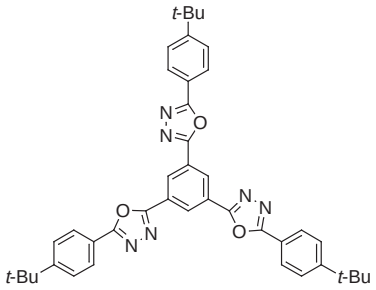

raphy, followed by recrystallisation from benzene–*n*-hexane to give colourless needles, and identified by various spectroscopies, mass spectrometry, and elemental analysis.[12,21,22]

Organic LEDs were fabricated by successive vacuum deposition of the organic materials onto an indium-tin-oxide (ITO)-coated glass substrate at a deposition rate of 2–3 Å s^{-1} at 10^{-5} Torr. Then, an alloy of magnesium and silver (volume ratio: *ca.* 10:1) was vacuum deposited onto the organic layer (thickness: *ca.* 1000 Å) by simultaneous evaporation from two separate sources. Current–voltage–luminance characteristics of the organic LEDs were measured with an electrometer (Advantest TR6143) and a luminance meter (Minolta LS-100). The electroluminescence and photoluminescence spectra were taken with a fluorescence spectrophotometer (Hitachi F-4500).

Results and discussion

Properties of BMA-*n*T

A novel class of organic π-electron systems, BMA-1T, BMA-2T, BMA-3T, and BMA-4T, readily form stable amorphous glasses with relatively high T_gs, when the melt samples are cooled. They form uniform amorphous films by vacuum deposition. Table 1 summarises the T_gs and molecular properties of BMA-*n*T (*n* = 1–4), *e.g.*, oxidation potentials ($E_{1/2}$), electronic absorption and fluorescence band maxima ($\lambda_{max}{}^a$ and $\lambda_{max}{}^f$) and fluorescence quantum efficiencies (Φ_f). The fluorescence band maxima of BMA-*n*T (*n* = 1–4) in tetrahydrofuran undergo significant red shift from 456 to 532 nm with increasing conjugation length of the oligothiophene moiety. The fluorescence quantum yields of BMA-*n*T (*n* = 1–4) in solution are in the range from 0.18 to 0.37. The half-wave oxidation potentials ($E_{1/2}$) of BMA-*n*T (*n* = 1–4) are relatively low, being in the range from 0.39 to 0.35 V *vs.* Ag/Ag^+ (0.01 mol dm^{-3}). BMA-*n*T (*n* = 1–4) possess electron-donating and hole-transporting properties (hole drift mobilities of BMA-3T and BMA-4T glasses: 2.8×10^{-5} and 1.0×10^{-5} cm^2 V^{-1} s^{-1}, respectively, at an electric field of 1.0×10^5 V cm^{-1} at 22 °C).[16] It is noteworthy that the half-wave oxidation potentials ($E_{1/2}$) of BMA-*n*T (*n* = 1–4) are almost the same irrespective of the conjugation length of the oligothiophene moiety but that the absorption edges of the electronic absorption bands of BMA-*n*T (*n* = 1–4) are significantly red-shifted with an increase in the conjugation length of the oligothiophene moiety. These results suggest that the ionisation potentials of BMA-*n*T (*n* = 1–4) are almost the same but that their electron affinities increase with increasing conjugation length of the oligothiophene moiety.

Table 1 Glass-transition temperatures (T_g), half-wave oxidation potentials ($E_{1/2}$), electronic absorption and fluorescence band maxima ($\lambda_{max}{}^a$ and $\lambda_{max}{}^f$), and fluorescence quantum efficiencies (Φ_f) of BMA-*n*T (*n* = 1–4)

Material	T_g/°C	$E_{1/2}$/V[a]	$\lambda_{max}{}^a$/nm[b]	$\lambda_{max}{}^f$/nm[b]	$\Phi_f{}^b$
BMA-1T	86	0.39	397	456	0.37
BMA-2T	90	0.39	423	491	0.19
BMA-3T	93	0.38	440	516	0.18
BMA-4T	98	0.35	453	532	0.22

[a] *vs.* Ag/Ag^+ in dichloromethane. [b] In tetrahydrofuran.

Fabrication of organic LEDs using BMA-*n*T

In our previous communication,[18] we have reported the fabrication and performances of single-layer devices using BMA-*n*T (*n* = 1–4) alone sandwiched between the ITO and MgAg electrodes. In the present study, we have fabricated double-layer devices consisting of the emitting layer of BMA-*n*T (*n* = 1–4) with hole-transporting properties and the electron-transport layer of Alq_3 or TPOB in order to improve the performances.

Fig. 1 shows the structure of the double-layer device together with that of the single-layer device. As observed for the single-layer devices, ITO/BMA-*n*T (*n* = 1–4) (1200 Å)/MgAg, the double-layer devices, ITO/BMA-*n*T (*n* = 2–4) (600 Å)/Alq_3

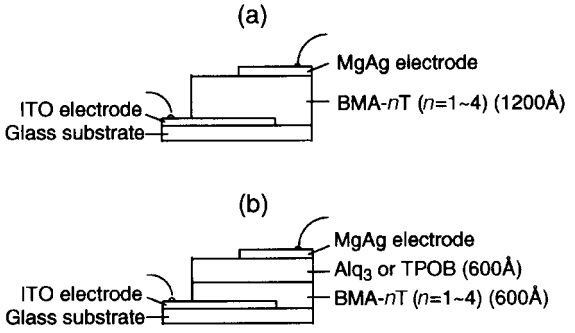

Fig. 1 Side views of (a) single-layer and (b) double-layer organic LEDs.

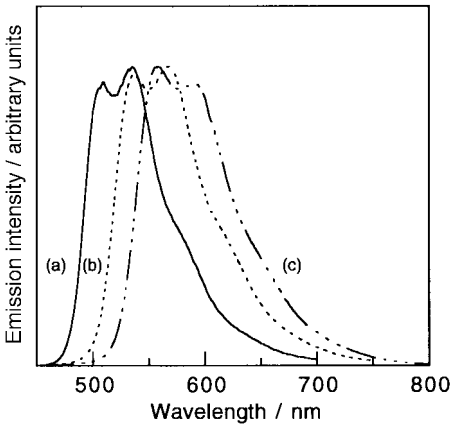

Fig. 2 Electroluminescence spectra for ITO/BMA-*n*T (n = 2–4)/Alq_3/MgAg double-layer organic LEDs; (a) BMA-2T, (b) BMA-3T, (c) BMA-4T.

(600 Å)/MgAg, showed rectification behaviour and emitted bright light when a positive voltage was applied to the ITO electrode.

Fig. 2 shows the electroluminescence (EL) spectra for the double-layer organic LEDs, ITO/BMA-*n*T (n = 2–4)/Alq_3/MgAg. Like the EL spectra for the single-layer organic LEDs using BMA-*n*T (n = 2–4) alone, the EL spectra for the double-layer devices were in accord with the photoluminescence (PL) (fluorescence) spectra of BMA-*n*T (n = 2–4) instead of Alq_3. The EL colour was yellowish green, yellow, and orange for the devices using BMA-2T, BMA-3T, and BMA-4T, respectively. This result indicates that BMA-*n*T (n = 2–4) and Alq_3 act as emitting materials and an electron-transporting material, respectively, in the double-layer devices and that the EL originates from the electronically excited singlet state of BMA-*n*T (n = 2–4). That is, electrons are injected from the MgAg electrode into the BMA-*n*T (n = 2–4) layer by a stepwise process through the Alq_3 layer, and then recombine with holes injected from the ITO electrode into the BMA-*n*T (n = 2–4) layer to generate the electronically excited singlet state of BMA-*n*T (n = 2–4).

It should be noted that the EL colour of the double-layer device consisting of BMA-1T and Alq_3, ITO/BMA-1T (600 Å)/Alq_3 (600 Å)/MgAg, was bluish white instead of the light blue obtained for the single-layer device using BMA-1T alone. As Fig. 3 shows, the emission from both Alq_3 and BMA-1T was observed for the double-layer device. This result indicates that holes are partly injected from the BMA-1T layer into the Alq_3 layer. In order to obtain light blue EL originating

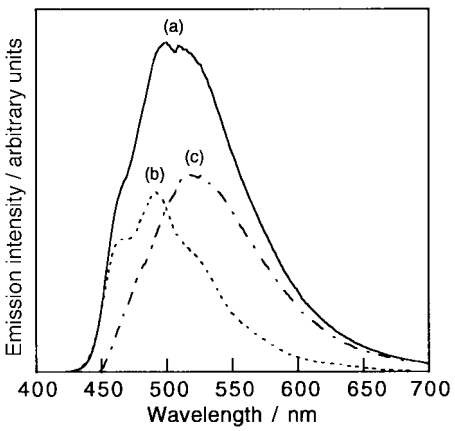

Fig. 3 Electroluminescence (EL) and photoluminescence (PL) spectra: (a) EL spectrum for ITO/BMA-1T/Alq_3/MgAg double-layer device; (b) and (c) PL spectra of the evaporated films of BMA-1T and Alq_3, respectively.

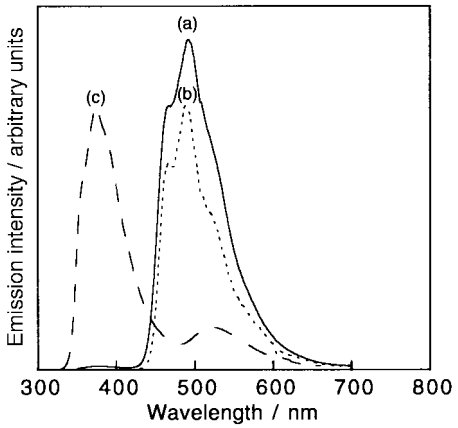

Fig. 4 Electroluminescence (EL) and photoluminescence (PL) spectra: (a) EL spectrum for ITO/BMA-1T/TPOB/MgAg double-layer device; (b) and (c) PL spectra of the evaporated films of BMA-1T and TPOB, respectively.

only from the electronically excited singlet state of BMA-1T, the electron-transporting material Alq_3 was replaced by TPOB. The reduction potential of TPOB is -2.1 V *vs.* Ag/Ag^+ (0.01 mol dm^{-3}), as determined by cyclic voltammetry in a tetrahydrofuran solution and the HOMO–LUMO energy gap of TPOB is estimated to be *ca.* 3.7 eV from the reduction potential and the electronic absorption edge. Since the HOMO–LUMO energy gap of TPOB is larger than those of BMA-1T (*ca.* 2.8 eV) and Alq_3 (*ca.* 2.7 eV), it is expected that the hole injection from the BMA-1T layer into the TPOB layer is prevented and that the recombination of holes and electrons takes place in the BMA-1T layer to generate the excited singlet state of BMA-1T. As Fig. 4 shows, a double-layer organic LED, ITO/BMA-1T (600 Å)/TPOB (600 Å)/MgAg, was found to emit bright blue light originating from BMA-1T.

Performances of organic LEDs using BMA-*n*T

The performances of the double-layer organic LEDs using BMA-*n*T (n = 1–4) as emitting materials and Alq_3 or TPOB as the electron-transporting material were examined and compared with those of the single-layer devices using BMA-*n*T (n = 1–4) alone.

First, the performances of the single-layer devices are described for the sake of comparison with the performances of the double-layer devices. Fig. 5 and 6 show injected current density–applied voltage and luminance–applied voltage characteristics for the single-layer organic LEDs using BMA-

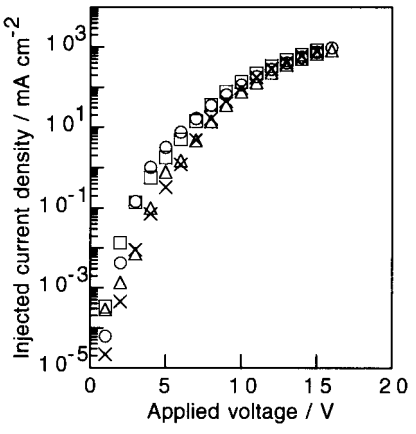

Fig. 5 Injected current density–applied voltage characteristics for ITO/BMA-*n*T (n = 1–4)/MgAg single-layer organic LEDs: × BMA-1T, △ BMA-2T, ○ BMA-3T, □ BMA-4T.

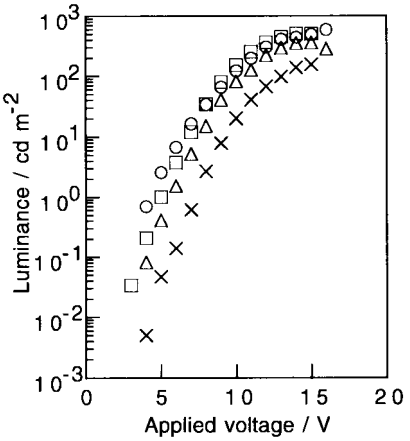

Fig. 6 Luminance–applied voltage characteristics for ITO/BMA-*n*T (*n* = 1–4)/MgAg single-layer organic LEDs: × BMA-1T, △ BMA-2T, ○ BMA-3T, □ BMA-4T.

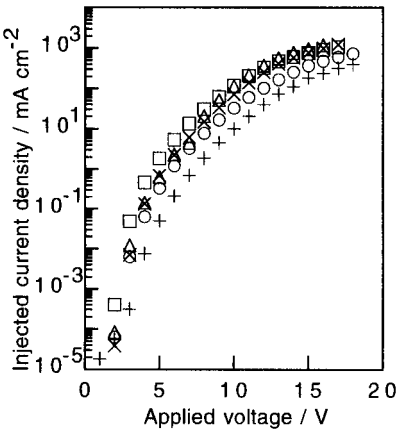

Fig. 7 Injected current density–applied voltage characteristics for ITO/BMA-*n*T (*n* = 1–4)/Alq_3 or TPOB/MgAg double-layer organic LEDs: + BMA-1T/TPOB, × BMA-1T/Alq_3, △ BMA-2T/Alq_3, ○ BMA-3T/Alq_3, □ BMA-4T/Alq_3.

*n*T alone. The emission started at a driving voltage of *ca.* 4 V for the device using BMA-1T, and *ca.* 3 V for the devices using BMA-2T, BMA-3T, and BMA-4T. The injected current density—applied voltage characteristics were similar for all the single-layer devices. This result indicates that an almost equal amount of the majority carrier, which is thought to be holes, is injected from the ITO electrode into the BMA-*n*T layer for all the single-layer organic LEDs. Therefore, the performances of the single-layer organic LEDs using BMA-*n*T (*n* = 1–4) alone are thought to be governed by the number of minority carriers, *i.e.*, electrons, injected from the MgAg electrode. In fact, the luminous and external quantum efficiencies for the single-layer organic LEDs were found to increase with increasing conjugation length of the oligothiophene moiety (Table 2). It is understood that the number of injected minority carriers, *i.e.*, electrons, increases with increasing conjugation length of the oligothiophene moiety due to a progressively decreased energy barrier for electron injection from the MgAg electrode into BMA-*n*T in going from *n* = 1 to *n* = 4.

The performances of the single-layer organic LEDs using emitting amorphous molecular materials, BMA-*n*T (*n* = 1–4), are much higher than those reported for the devices using polycrystalline films or LB films of oligothiophenes as emitting materials.[29–32] It has been reported that the fluorescence quantum efficiencies (Φ) of unsubstituted and α,α′-disubstituted oligothiophenes in their polycrystalline films ($\Phi = ca.\ 10^{-3}$ for the α-oligothiophenes with 4–8 rings)[35] are much lower than those in their solutions ($\Phi = 1.8 \times 10^{-1}$–$3.4 \times 10^{-1}$ for the α-oligothiophenes with 4–7 rings in dioxane)[36] and single crystals ($\Phi = 4 \times 10^{-2}$ for the α-octithiophene)[37] because of the close-packed arrangement of the molecules and the disordered domains.[35,37–39] It is thought that the enhanced performances of the devices using amorphous BMA-*n*T (*n* = 1–4) relative to the performances of the devices using polycrystalline oligothiophenes are due to much higher fluorescence quantum efficiencies of BMA-*n*T in their amorphous films (in which the close-packed arrangement of the molecules is prevented due to the substitution with the nonplanar bulky group), relative to those of oligothiophenes in their polycrystalline films. The good quality of the amorphous thin films of BMA-*n*T is also a factor.

Next, the performances of the double-layer devices are described and compared with those of the single-layer devices. Fig. 7 and 8 show the injected current density–applied voltage and luminance–applied voltage characteristics for the double-layer organic LEDs using BMA-*n*T (*n* = 1–4) as the emitting layer and Alq_3 or TPOB as the electron-transport layer. The emission started at a driving voltage of *ca.* 3 V for the double-layer devices. Table 3 summarises the maximum luminances, luminous efficiencies, and external quantum efficiencies of EL for the double-layer devices. The double-layer organic LEDs consisting of the emitting layer of BMA-*n*T (*n* = 2–4) and the electron-transport layer of Alq_3 showed performances more than one order of magnitude higher than the corresponding single-layer organic LEDs, as clearly seen in Fig. 9. The double-layer device, *e.g.*, ITO/BMA-2T (600 Å)/Alq_3 (600 Å)/MgAg, exhibited a maximum luminance of 15000 cd m^{-2} at a driving voltage of 16 V and a luminous efficiency of 1.5 lm W^{-1} at a luminance of 300 cd m^{-2}. The double-layer organic LEDs using BMA-1T and TPOB as the electron-transport layer also showed luminous and quantum

Table 2 Performances of single-layer organic LEDs, ITO/BMA-*n*T (*n* = 1–4) (1200 Å)/MgAg EL devices

Material	Maximum luminance[a] /cd m^{-2}	Luminous efficiency[c] /lm W^{-1}	Quantum efficiency[c] (%)
BMA-1T	160	0.004[d]	0.009[d]
BMA-2T	360	0.020	0.024
BMA-3T	600[b]	0.027	0.032
BMA-4T	510	0.030	0.040

[a]At 15 V. [b]At 16 V. [c]For obtaining 300 cd m^{-2}. [d]For obtaining 160 cd m^{-2}.

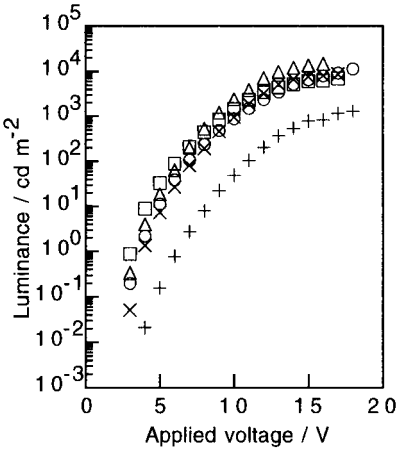

Fig. 8 Luminance–applied voltage characteristics for the ITO/BMA-*n*T (*n* = 1–4)/Alq_3/MgAg double-layer organic LEDs: + BMA-1T/TPOB, × BMA-1T/Alq_3, △ BMA-2T/Alq_3, ○ BMA-3T/Alq_3, □ BMA-4T/Alq_3.

Table 3 Performances of the double-layer organic LEDs, ITO/BMA-*n*T ($n=1$–4) (600 Å)/Alq_3 (600 Å)/MgAg and ITO/BMA-1T (600 Å)/TPOB (600 Å)/MgAg

Material	Maximum luminance /cd m^{-2}	Luminous efficiency[d] /lm W^{-1}	Quantum efficiency[d] (%)
BMA-1T/TPOB	1300[a]	0.13	0.22
BMA-1T/Alq_3	8800[b]	0.50	0.49
BMA-2T/Alq_3	15000[c]	1.5	0.90
BMA-3T/Alq_3	13000[a]	1.1	0.90
BMA-4T/Alq_3	7000[b]	0.70	0.53

[a]At 18 V. [b]At 17 V. [c]At 16 V. [d]For obtaining 300 cd m^{-2}.

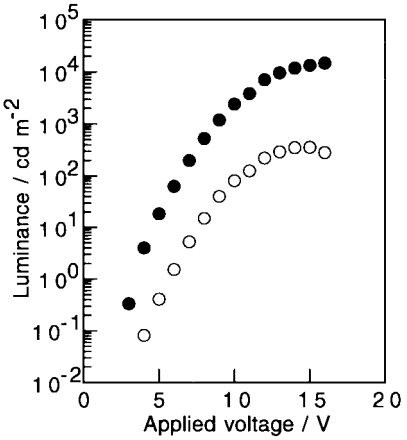

Fig. 9 Luminance–applied voltage characteristics for ITO/BMA-2T/MgAg single-layer organic LED (○) and ITO/BMA-2T/Alq_3/MgAg double-layer organic LED (●).

efficiencies more than one order of magnitude higher than the single-layer device using BMA-1T alone.

It is suggested that in the double-layer devices, electron injection from the MgAg electrode into the BMA-*n*T ($n=1$–4) layer becomes more efficient due to a decreased energy barrier in the presence of the electron-transport layer. In addition, the presence of the electron-transport layer of Alq_3 or TPOB acts as a blocking layer for the hole injection from BMA-*n*T into Alq_3 or TPOB, reducing the number of holes travelling to the cathode. As a result, a better balance of the number of holes and electrons injected is attained; this is responsible for much better performances for the double-layer organic LEDs than for the single-layer devices.

The present study shows that a novel class of amorphous molecular materials with hole-transporting properties, BMA-*n*T ($n=1$–4), function as excellent colour-tunable emitting materials for organic LEDs and that the double-layer devices consisting of the emitting layer of BMA-*n*T ($n=1$–4) and the electron-transport layer of Alq_3 and TPOB exhibit high performances.

Conclusion

A novel family of amorphous molecular materials containing an oligothiophene moiety with varying conjugation length, BMA-*n*T ($n=1$–4), function as thermally and morphologically stable, colour-tunable emitting materials for organic LEDs. Tuning of the emission colour from light blue to orange is achieved by varying the conjugation length of the oligothiophene moiety.

Both the single layer devices using BMA-*n*T ($n=1$–4) alone and double-layer devices consisting of the emitting layer of BMA-*n*T ($n=1$–4) with hole-transporting properties and the electron-transport layer of Alq_3 or TPOB exhibit higher performances than the devices using polycrystalline oligothiophenes. The double-layer devices exhibit performances more than one order of magnitude higher than the single-layer devices.

References

1 C. W. Tang and S. A. VanSlyke, *Appl. Phys. Lett.*, 1987, **51**, 913.
2 P. L. Burn, A. B. Holmes, A. Karft, D. D. C. Bradley, A. R. Brown, R. H. Friend and R. W. Gymer, *Nature*, 1992, **356**, 47.
3 Y. Shirota, *Proc. SPIE Int. Soc. Opt. Eng.*, 1997, **3148**, 186 and references cited therein.
4 Y. Shirota, T. Kobata and N. Noma, *Chem. Lett.*, 1989, 1145.
5 A. Higuchi, K. Ohnishi, S. Nomura, H. Inada and Y. Shirota, *J. Mater. Chem.*, 1992, **2**, 1109.
6 W. Ishikawa, H. Inada, H. Nakano and Y. Shirota, *Mol. Cryst. Liq. Cryst.*, 1992, **211**, 431.
7 W. Ishikawa, K. Noguchi, Y. Kuwabara and Y. Shirota, *Adv. Mater.*, 1993, **5**, 559.
8 H. Inada, K. Ohnishi, S. Nomura, A. Higuchi, H. Nakano and Y. Shirota, *J. Mater. Chem.*, 1994, **4**, 171.
9 Y. Shirota, Y. Kuwabara, H. Inada, T. Wakimoto, H. Nakada, Y. Yonemoto, S. Kawami and K. Imai, *Appl. Phys. Lett.*, 1994, **65**, 807.
10 Y. Kuwabara, H. Ogawa, H. Inada, N. Noma and Y. Shirota, *Adv. Mater.*, 1994, **6**, 677.
11 H. Inada, Y. Yonemoto, T. Wakimoto, K. Imai and Y. Shirota, *Mol. Cryst. Liq. Cryst.*, 1996, **280**, 331.
12 Y. Shirota, Y. Kuwabara, D. Okuda, R. Okuda, H. Ogawa, H. Inada, T. Wakimoto, H. Nakada, Y. Yonemoto, S. Kawami and K. Imai, *J. Lumin.*, 1997, **72–74**, 985.
13 K. Itano, T. Tsuzuki, H. Ogawa, S. Appleyard, M. R. Willis and Y. Shirota, *IEEE Trans. Electron Devices*, 1997, **44**, 1218.
14 H. Ogawa, H. Inada and Y. Shirota, *Macromol. Symp.*, 1997, **125**, 171.
15 H. Ogawa, K. Ohnishi and Y. Shirota, *Synth. Met.*, 1997, **91**, 243.
16 T. Noda, I. Imae, N. Noma and Y. Shirota, *Adv. Mater.*, 1997, **9**, 239.
17 T. Noda, H. Ogawa, N. Noma and Y. Shirota, *Appl. Phys. Lett.*, 1997, **70**, 699.
18 T. Noda, H. Ogawa, N. Noma and Y. Shirota, *Adv. Mater.*, 1997, **9**, 720.
19 K. Katsuma and Y. Shirota, *Adv. Mater.*, 1998, **10**, 223.
20 K. Itano, H. Ogawa and Y. Shirota, *Appl. Phys. Lett.*, 1998, **72**, 636.
21 H. Ogawa, R. Okuda and Y. Shirota, *Mol. Cryst. Liq. Cryst.*, 1998, **315**, 489.
22 H. Ogawa, R. Okuda and Y. Shirota, *Appl. Phys. A*, 1998, **67**, 599.
23 T. Noda and Y. Shirota, *J. Am. Chem. Soc.*, 1998, **120**, 9714.
24 T. Noda, H. Ogawa and Y. Shirota, *Adv. Mater.*, 1999, **11**, 283.
25 Y. Hamada, T. Sano, M. Fujita and T. Fujii, *Chem. Lett.*, 1993, 905.
26 C. Hosokawa, H. Higashi, H. Nakamura and T. Kusumoto, *Appl. Phys. Lett.*, 1995, **67**, 3853.
27 J. Kido, M. Kimura and K. Nagai, *Chem. Lett.*, 1996, 47.
28 J. Salbeck, N. Yu, J. Bauer, F. Weissörtel and H. Bestgen, *Synth. Met.*, 1997, **91**, 209.
29 K. Uchiyama, H. Akimichi, S. Hotta, H. Noge and H. Sakaki, *Synth. Met.*, 1994, **63**, 57.
30 F. Geiger, M. Stoldt, H. Schweizer, P. Bäuerle and E. Umbach, *Adv. Mater.*, 1993, **5**, 922.
31 G. Horowitz, P. Delannoy, H. Bouchriha, F. Deloffre, J.-L. Fave, F. Garnier, R. Hajlaoui, M. Heyman, F. Kouki, P. Valat, V. Wintgens and A. Yassar, *Adv. Mater.*, 1994, **6**, 752.
32 A. J. Pal, J. Paloheimo and H. Stubb, *Appl. Phys. Lett.*, 1995, **67**, 3909.
33 B. Servet, S. Ries, M. Trotel, P. Alnot, G. Horowitz and F. Garnier, *Adv. Mater.*, 1993, **5**, 461.
34 S. Hotta and K. Waragai, *Adv. Mater.*, 1993, **5**, 896.
35 D. Oelkrug, H.-J. Egelhaaf, D. R. Worrall and F. Wilkinson, *J. Fluoresc.*, 1995, **5**, 165.
36 R. S. Becker, J. Seixas de Melo, A. L. Maçanita and F. Elisei, *J. Phys. Chem.*, 1996, **100**, 18683.
37 D. Moses, J. Wang, A. Dogariu, D. Fichou and C. Videlot, *Phys. Rev. B.*, 1999, **59**, 7715.
38 A. Yassar, G. Horowitz, P. Valat, V. Wintgens, M. Hmyene, F. Deloffre, P. Srivastava, P. Lang and F. Garnier, *J. Phys. Chem.*, 1995, **99**, 9155.
39 R. N. Marks, R. H. Michel, W. Gebauer, R. Zamboni, C. Taliani, R. F. Mahrt and M. Hopmeier, *J. Phys. Chem. B*, 1998, **102**, 7563.

Paper 9/02800E